Electronic Supplementary Material (ESI) for Analyst

Supplementary data

A coumarin-indole-based near-infrared ratiometric pH probe for intracellular fluorescence imaging

Xiao-Dong Liu,[a] Ying Xu,[b] Ru Sun,[*c] Yu-Jie Xu,[b] Jian-Mei Lu,[*a] Jian-Feng Ge[*a]

[a] *Key Laboratory of Organic Synthesis of Jiangsu Province, Soochow University, 199 Ren'Ai Road, Suzhou 215123, China. E-mail: lujm@suda.edu.cn; ge_jianfeng@hotmail.com.*

[b] *School of Radiation Medicine and Protection, Medicine College of Soochow University, Suzhou 215123, China.*

[c] *College of Chemistry, Chemical Engineering and Material Science, Soochow University, 199 Ren'Ai Road, Suzhou 215123, China. E-mail: sunru924@hotmail.com.*

Index

1 Figures

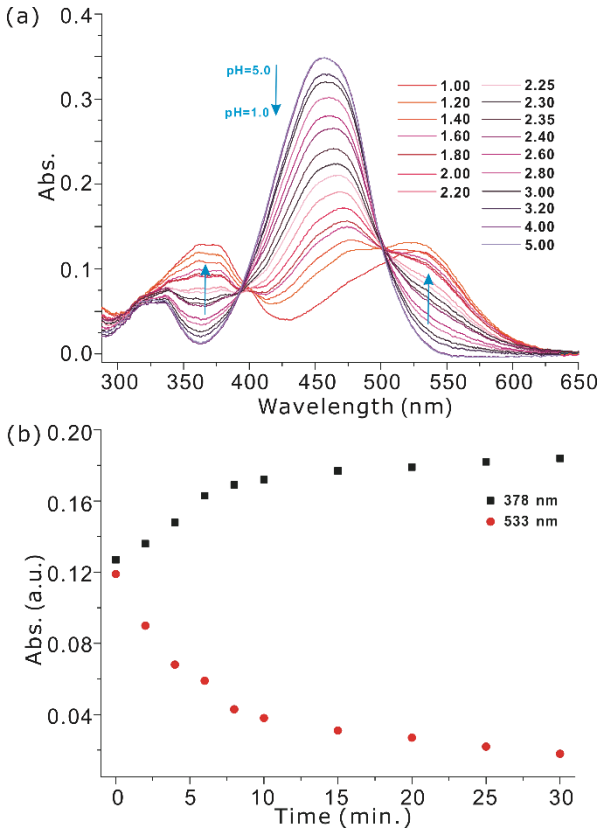

Fig. S1 Absorption properties of probe **1** (10 μM) with different pH in acetonitrile-buffer (v:v = 1:4) solution. (a) Instant absorption spectra within 1 min; (b) Time depended absorption intensity at 378 and 533 nm (pH = 1.0).

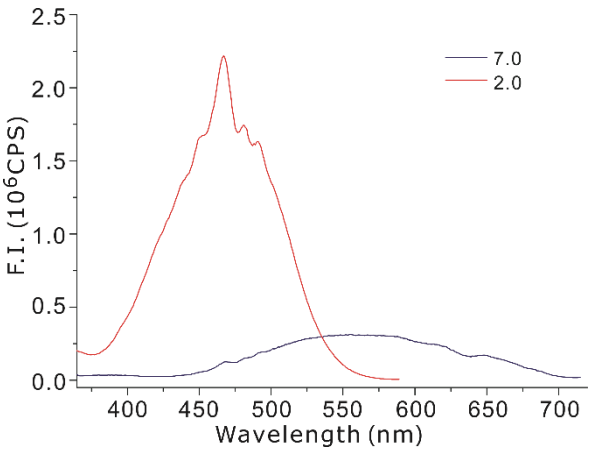

Fig. S2 Excitation spectra of probe **3** (10 μM). Red line: at pH 2.0, λ_{em} = 600 nm; black line: at pH 7.0, λ_{em} = 722 nm. Conditions: acetonitrile – Na_2HPO_4-citric acid buffer solution (20 mM, 3:7, v/v, rt).

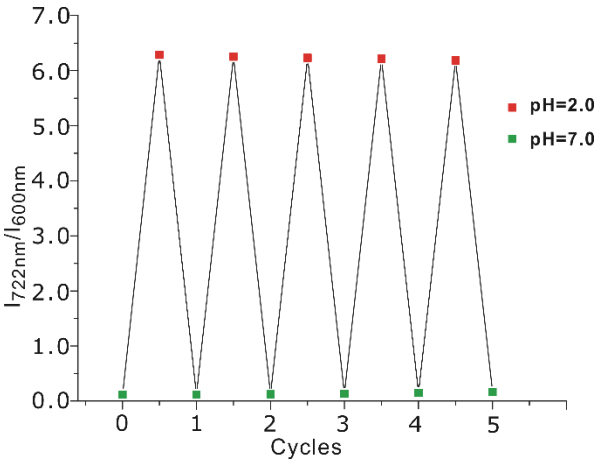

Fig. S3 The emission ratios of probe **3** at I_{722nm}/I_{600nm}, pH was changed alternately between 2.0 and 7.0.

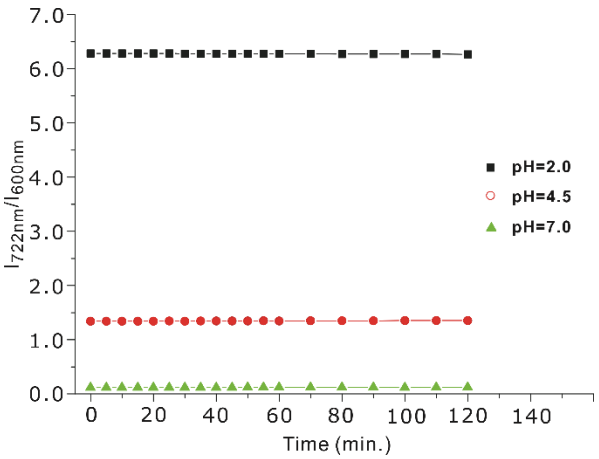

Fig. S4 Changes in the emission ratios at I_{722nm}/I_{600nm} for probe **3** with time at pH 2.0, 4.5, 7.0. Conditions: acetonitrile – Na_2HPO_4-citric acid buffer solution (20 mM, 3:7, v/v, rt), λ_{ex} = 540 nm.

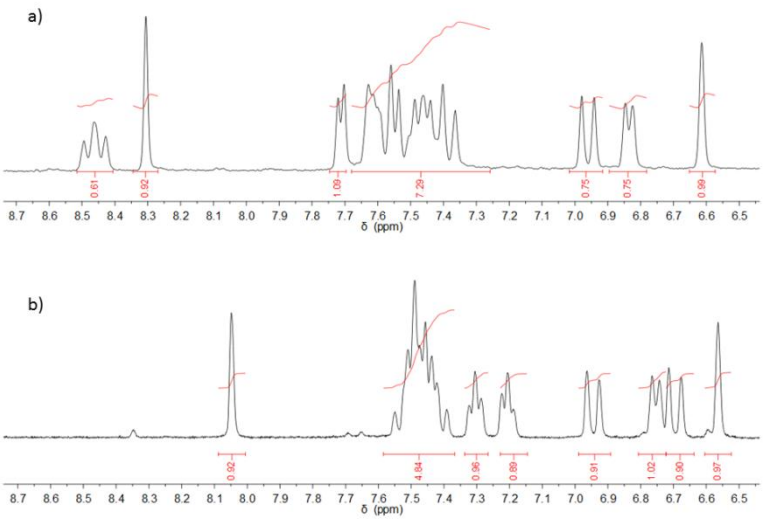

Fig. S5 ^{1}H NMR spectral changes of **3** (10 mM in DMSO-*d6*) in the presence (a) and absence (b) of hydrochloric acid.

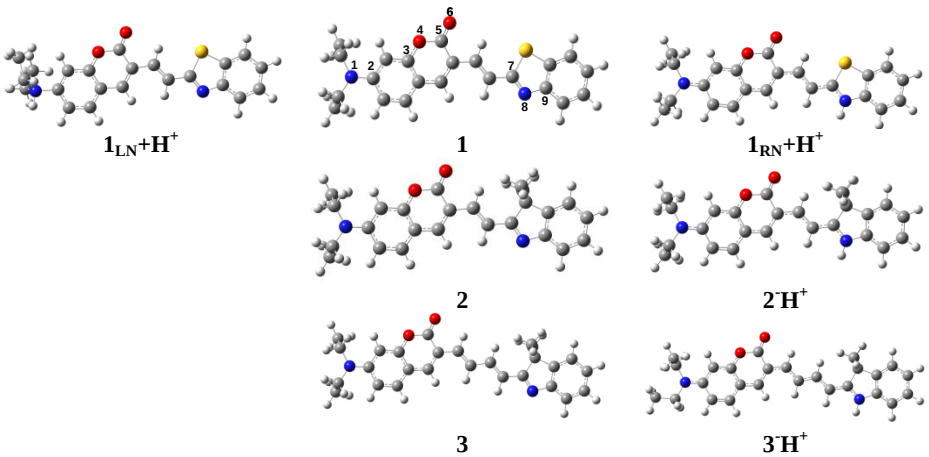

Fig. S6 The optimized structures of probes **1-3** and their protonated forms determined by DFT calculations.

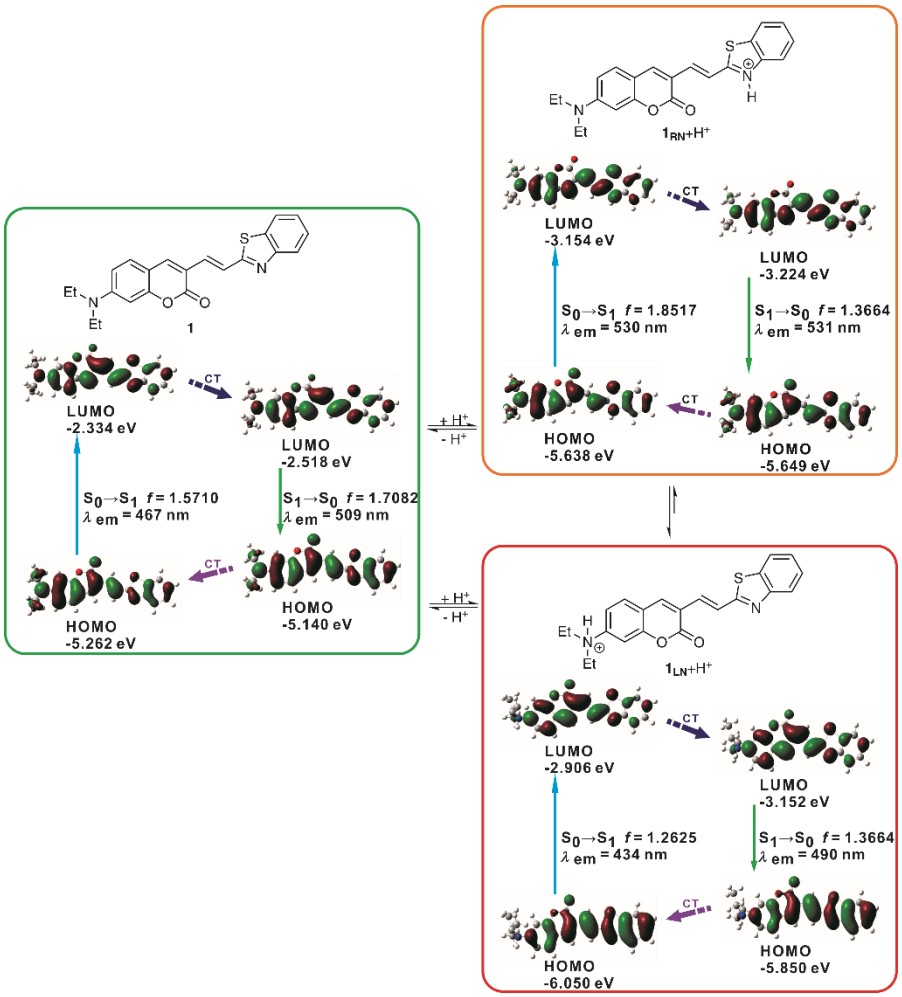

Fig. S7 The frontier molecular orbitals (FMOs) involved in the vertical excitation and emission of probe **1** and **1+H**$^+$. CT stands for conformation transformation. Excitation and radiative processes are marked as solid lines and the non-radiative processes are marked by dotted lines. For details please refer to Table S2 and S3.

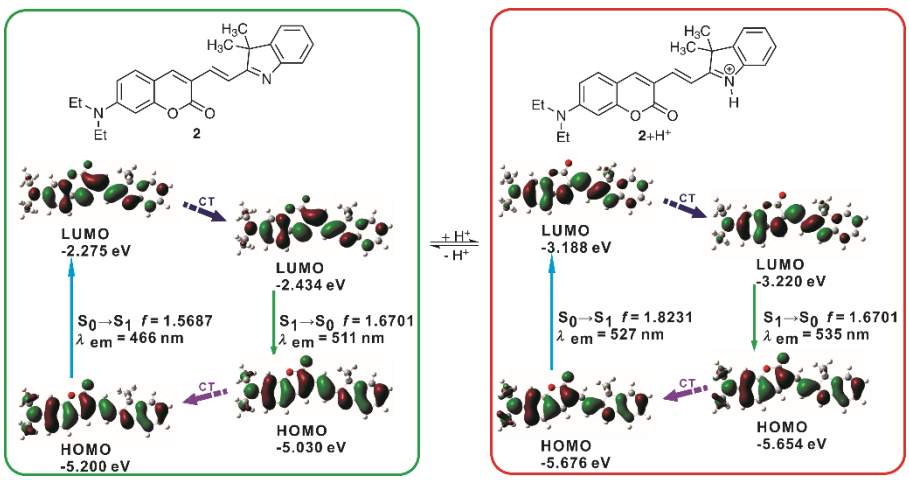

Fig. S8 The frontier molecular orbitals (FMOs) involved in the vertical excitation and emission of probe **2** and **2+H**$^+$. CT stands for conformation transformation. Excitation and radiative processes are marked as solid lines and the non-radiative processes are marked by dotted lines. For details please refer to Table S2 and S3.

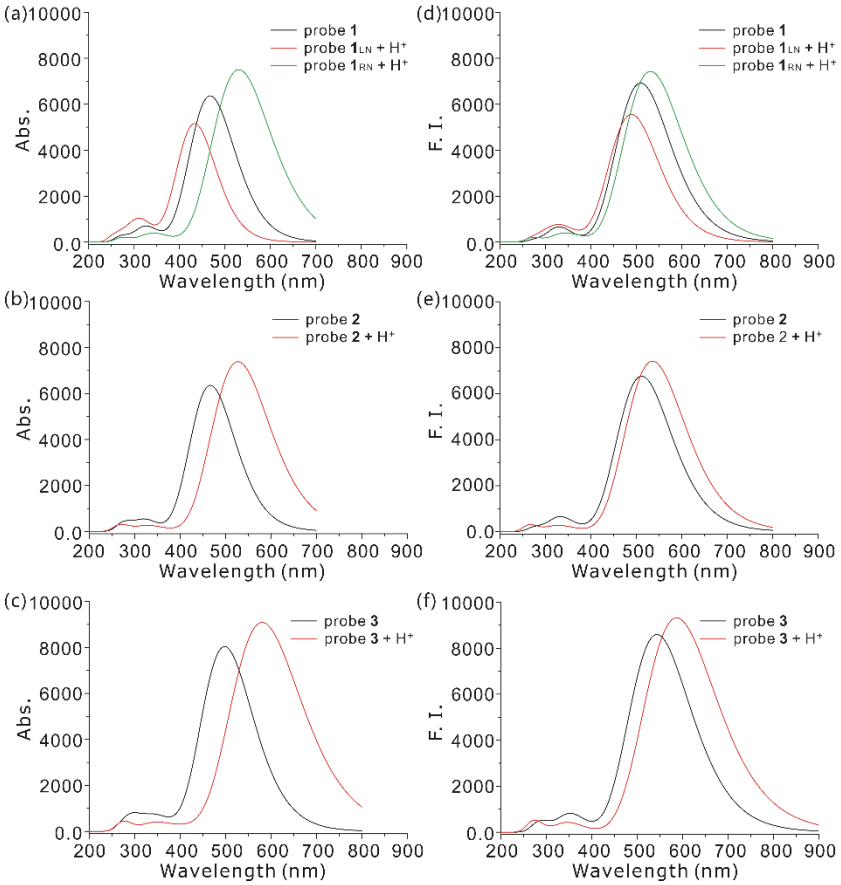

Fig. S9 The simulated UV-Vis and emission spectra based on TDDFT for probes **1-3** and their protonated forms.

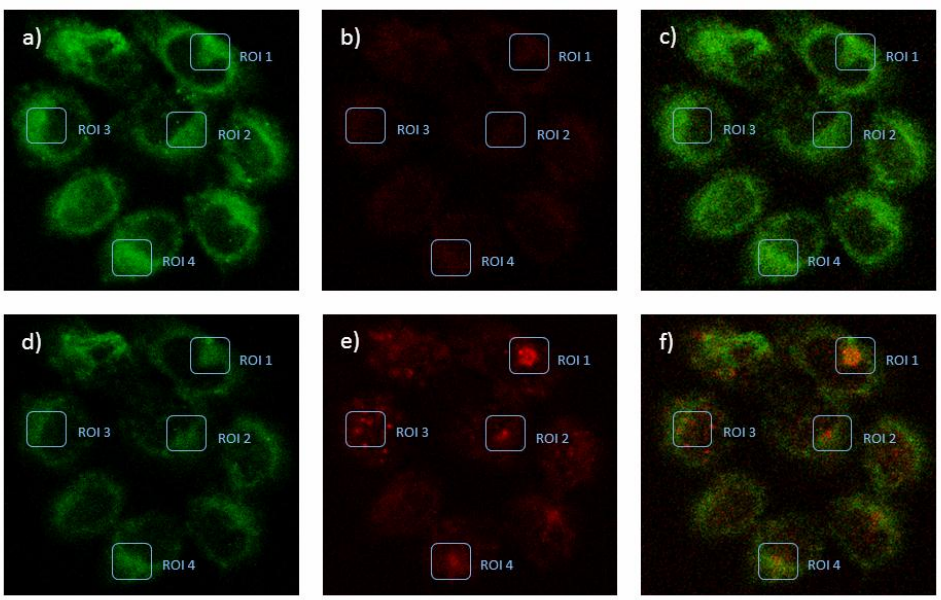

Fig. S10 Fluorescence images of probe **3** in living KB cells corresponding to Fig. 6. Four areas (ROI 1-4) in the images were chosen to represent the lysosomal regions of the KB cells.

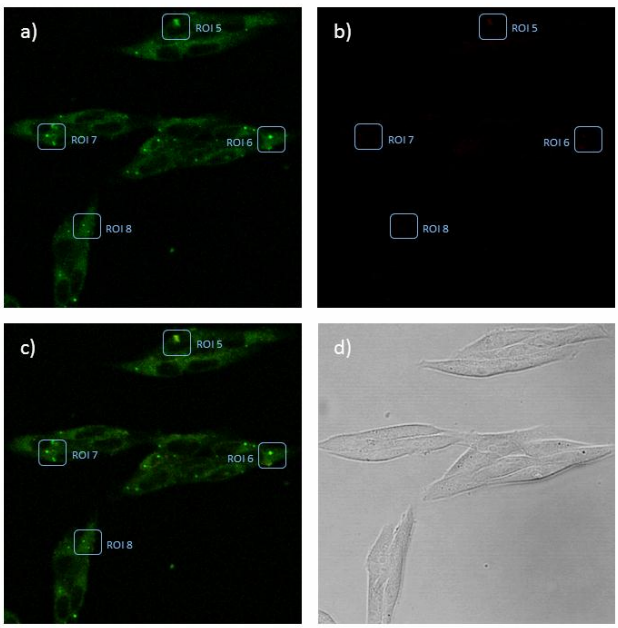

Fig. S11 Fluorescence images of living V79 cells. (1) Fluorescence images of V79 cells stained with probe **3** (10 μM) at 37 ºC for 10 min, (a) and (b) were collected at λ_{ex} = 488 nm and 633 nm respectively; (c) merged image of green (a) and red (b) channels; (d) bright-field transmission image of the cells. Four areas (ROI 5-8) in the images were chosen to represent the lysosomal regions of the V79 cells.

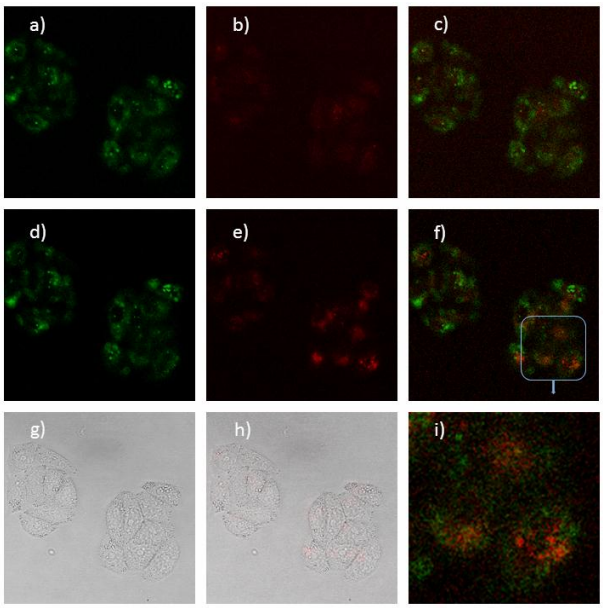

Fig. S12 Fluorescence images of living HeLa cells. (1) Fluorescence images of HeLa cells stained with probe **3** (10 μM) at 37 ºC for 10 min, (a) and (b) were collected at λ_{ex} = 488 nm and 633 nm respectively; (c) merged image of green (a) and red (b) channels; (2) fluorescence images of HeLa cells in (a) and (b) followed by further treatment with 1 mM ATP solution for 3 min. (d) and (e) were collected at λ_{ex} = 488 nm and 633 nm respectively; (f) merged image of green (d) and red (e) channels; (g) bright-field transmission image of the cells; (h) merged image of (e) and (g); (i) Partial enlarged image of (f).

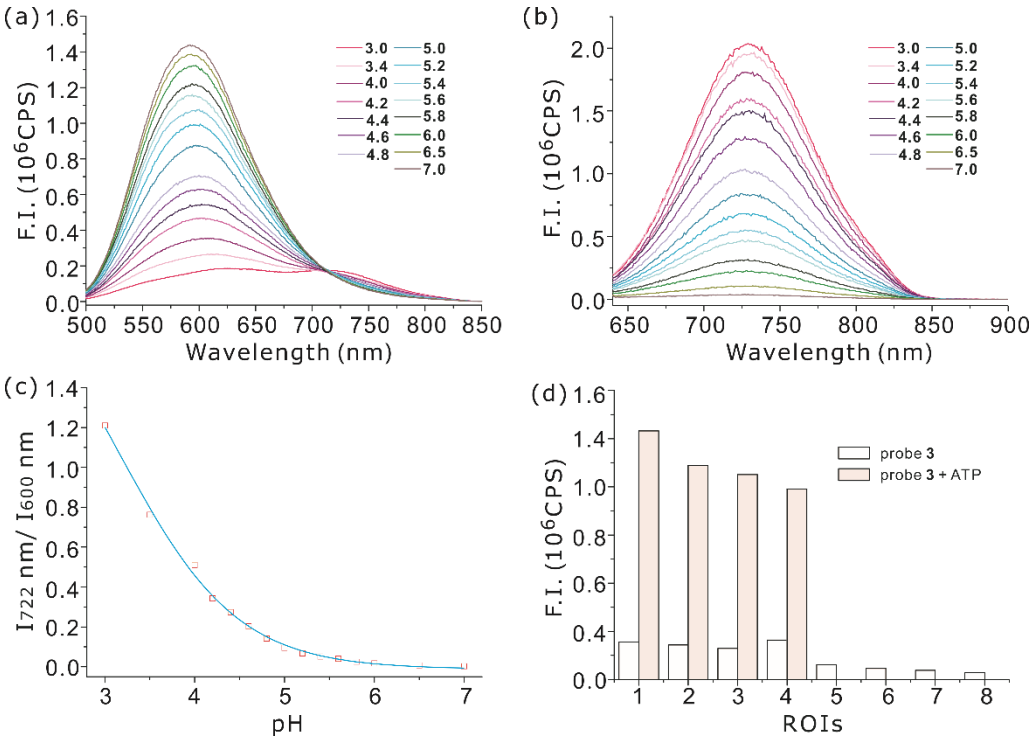

Fig. S13 (a) Emission spectra (λ_{ex} = 488 nm) of probes **3** (10 μM) with different pH in acetonitrile-buffer (v:v = 3:7) solution. (b) Emission spectra (λ_{ex} = 633 nm) of probes **3** (10 μM) with different pH in acetonitrile-buffer (v:v = 3:7) solution. (c) pH depended plot of the emission intensity at I_{722nm}/I_{600nm} which was obtained by calculating the ratios of fluorescence intensities at 722 nm (λ_{ex} = 633 nm) to that at 600 nm (λ_{ex} = 488 nm).(d) Relative fluorescence intensity ratios of the red channel to green channel in ROI 1-8 of KB and V79 cells.

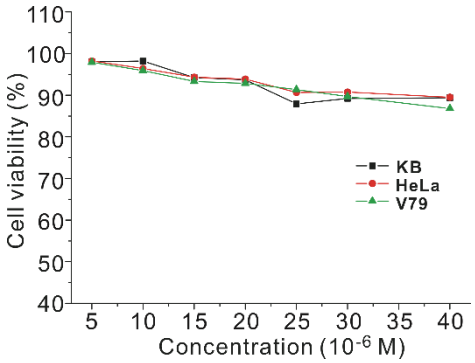

Fig. S14 Cytotoxicity of probe **3** on KB, HeLa and V79 cells. Cell viability was assayed by the MTT method.

2 Tables

Table S1. Selected C-N or C-O bond lengths (in Å) of probes **1-3** and their protonated forms determined by DFT calculations.

Probes	N1-C2	C3-O4	O4-C5	C5-O6	C7-N8	N8-C9
$\mathbf{1_{LN}+H^+}$	1.488	1.353	1.403	1.201	1.308	1.374
$\mathbf{1_{RN}+H^+}$	1.355	1.361	1.392	1.206	1.352	1.395
1	1.379	1.364	1.394	1.210	1.305	1.380
$\mathbf{2+H^+}$	1.355	1.362	1.391	1.207	1.343	1.409
2	1.380	1.365	1.393	1.211	1.308	1.404
$\mathbf{3+H^+}$	1.361	1.362	1.392	1.206	1.347	1.408
3	1.380	1.365	1.394	1.210	1.309	1.404

Table S2 Selected parameters for the vertical excitation (UV-vis absorptions) of the probes **1-3** and their protonated forms based on the optimized ground state geometries.

Compound	Electronic transitions	Excitation energy(eV)[a]	Exp.[b]	f[c]	Composition[d]	CI[e]
$\mathbf{1_{LN}+H^+}$	$S_0 \rightarrow S_1$	2.86(434nm)	378	1.2625	H→L	0.70469
$\mathbf{1_{RN}+H^+}$	$S_0 \rightarrow S_1$	2.34(530nm)	533	1.8517	H→L	0.70731
1	$S_0 \rightarrow S_1$	2.65(467nm)	460	1.5710	H→L	0.70558
$\mathbf{2+H^+}$	$S_0 \rightarrow S_1$	2.35(527nm)	559	1.8231	H→L	0.70632
2	$S_0 \rightarrow S_1$	2.66(466nm)	469	1.5687	H→L	0.70624
$\mathbf{3+H^+}$	$S_0 \rightarrow S_1$	2.14(580nm)	572	2.2444	H→L	0.70917
3	$S_0 \rightarrow S_1$	2.49(498nm)	474	1.9844	H→L	0.70661

[a] Electronic excitation energies (eV), The numbers in parentheses are the excitation energy in wavelength. [b] The experimental values. [c] Oscillator strength. [d] H stands for HOMO and L stands for LUMO. [e] Coefficient of the wavefunction for each excitations. The CI coefficients are in absolute values.

Table S3 Selected parameters for emission related of the probes **1-3** and their protonated forms based on the optimized lowest singlet excited state geometries.

Compound	Electronic transitions	Excitation energy(eV)[a]	Exp.[b]	f[c]	Composition[d]	CI[e]
$\mathbf{1_{LN}+H^+}$	$S_1 \rightarrow S_0$	2.53(490nm)	410	1.3664	L→H	0.70805
$\mathbf{1_{RN}+H^+}$	$S_1 \rightarrow S_0$	2.33(531nm)	-	1.8332	L→H	0.70733
1	$S_1 \rightarrow S_0$	2.43(509nm)	536	1.7082	L→H	0.70846
$\mathbf{2+H^+}$	$S_1 \rightarrow S_0$	2.32(535nm)	648	1.8309	L→H	0.70709
2	$S_1 \rightarrow S_0$	2.42(511nm)	562	1.6701	L→H	0.70919
$\mathbf{3+H^+}$	$S_1 \rightarrow S_0$	2.11(586nm)	722	2.3019	L→H	0.71023
3	$S_1 \rightarrow S_0$	2.28(543nm)	600	2.1227	L→H	0.70929

[a] Electronic excitation energies (eV), The numbers in parentheses are the excitation energy in wavelength. [b] The experimental values. [c] Oscillator strength. [d] H stands for HOMO and L stands for LUMO. [e] Coefficient of the wavefunction for each excitations. The CI coefficients are in absolute values.

3 Appendix

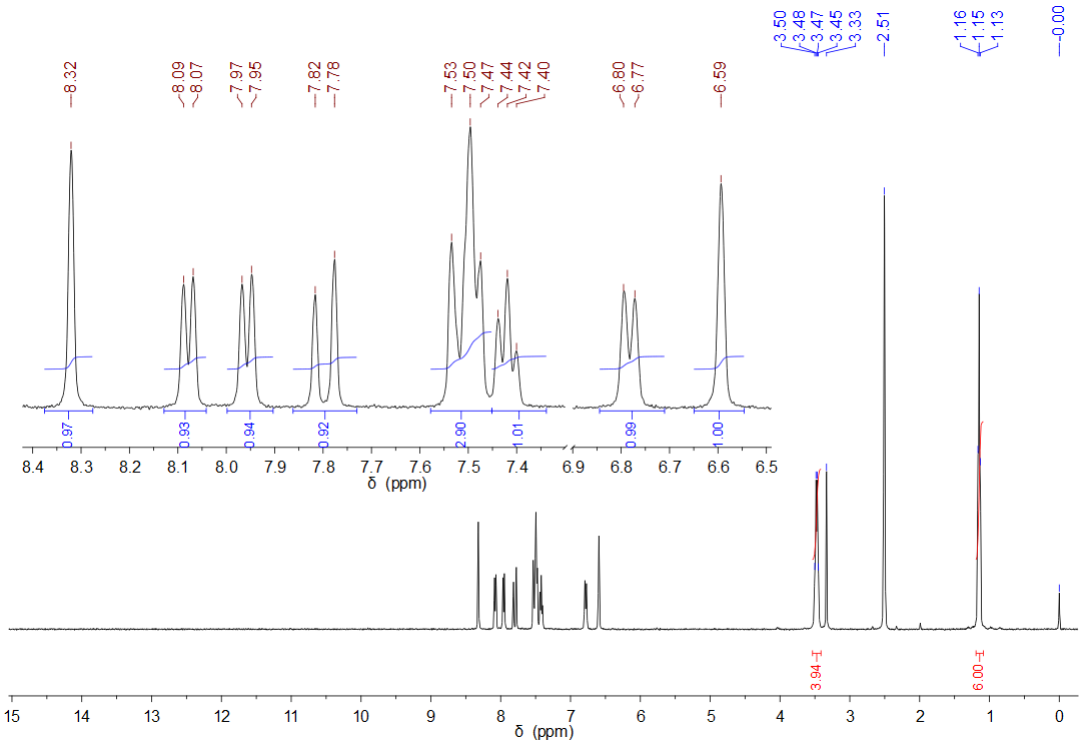

Fig. S15 ^{1}H NMR spectrum of **1** in DMSO-d_6.

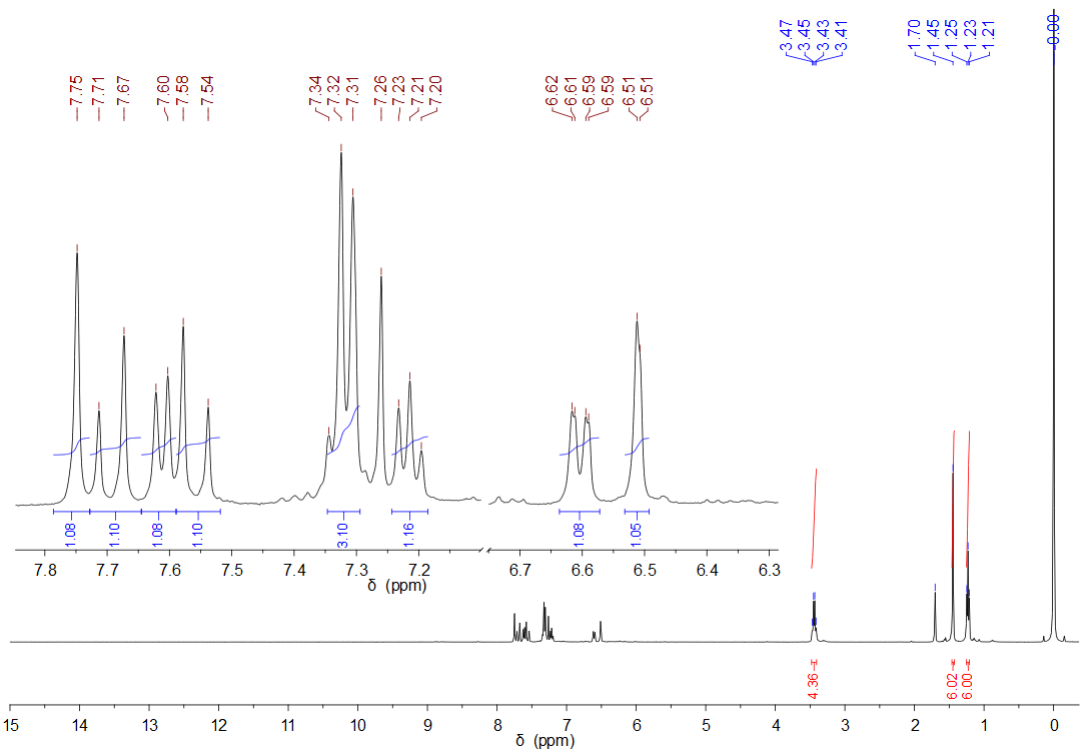

Fig. S16 ^{1}H NMR spectrum of **2** in $CDCl_3$.

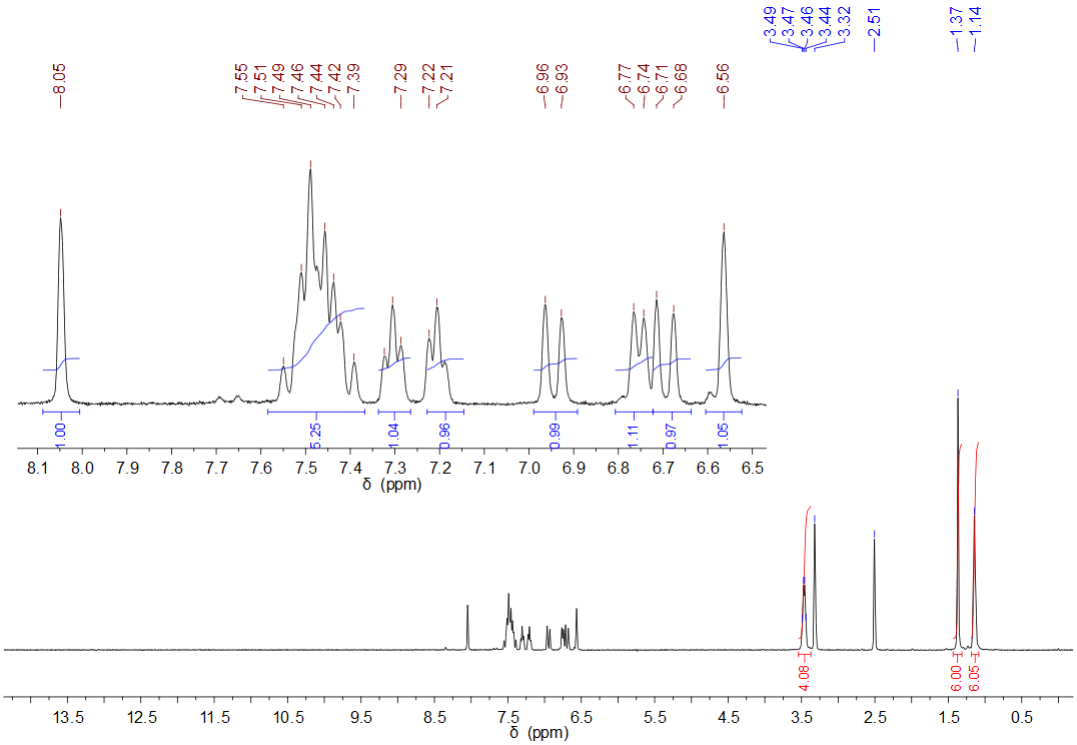

Fig. S17 ^{1}H NMR spectrum of **3** in DMSO-d_6.

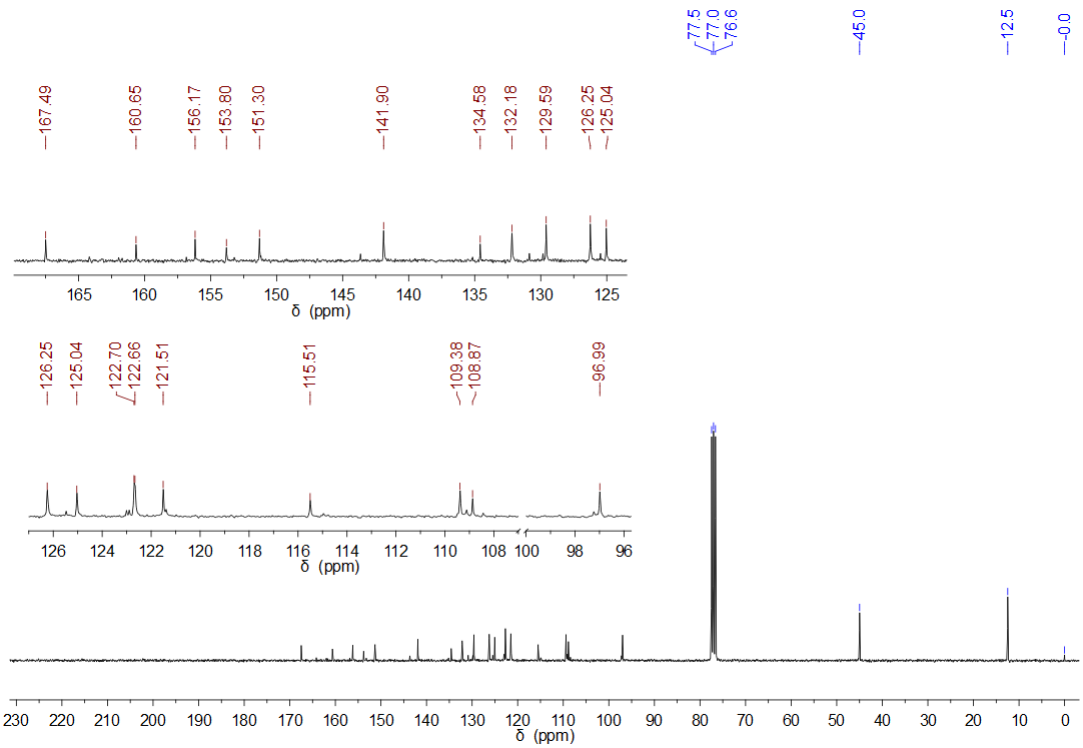

Fig. S18 ^{13}C NMR spectrum of **1** in $CDCl_3$.

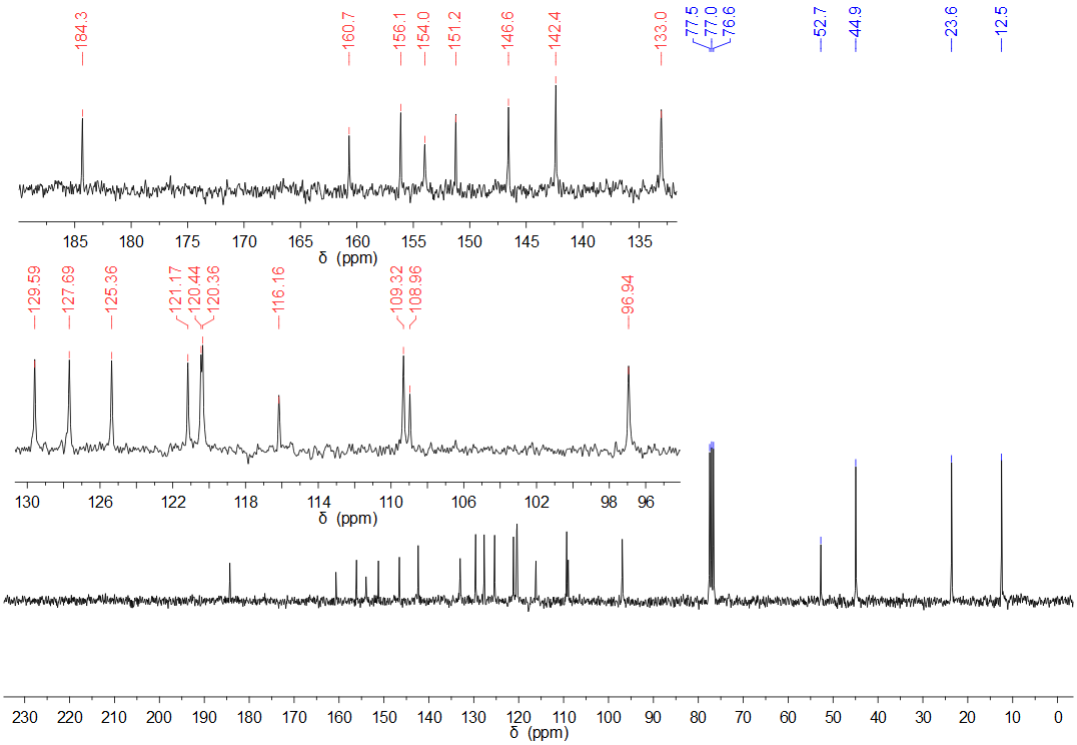

Fig. S19 ^{13}C NMR spectrum of **2** in $CDCl_3$.

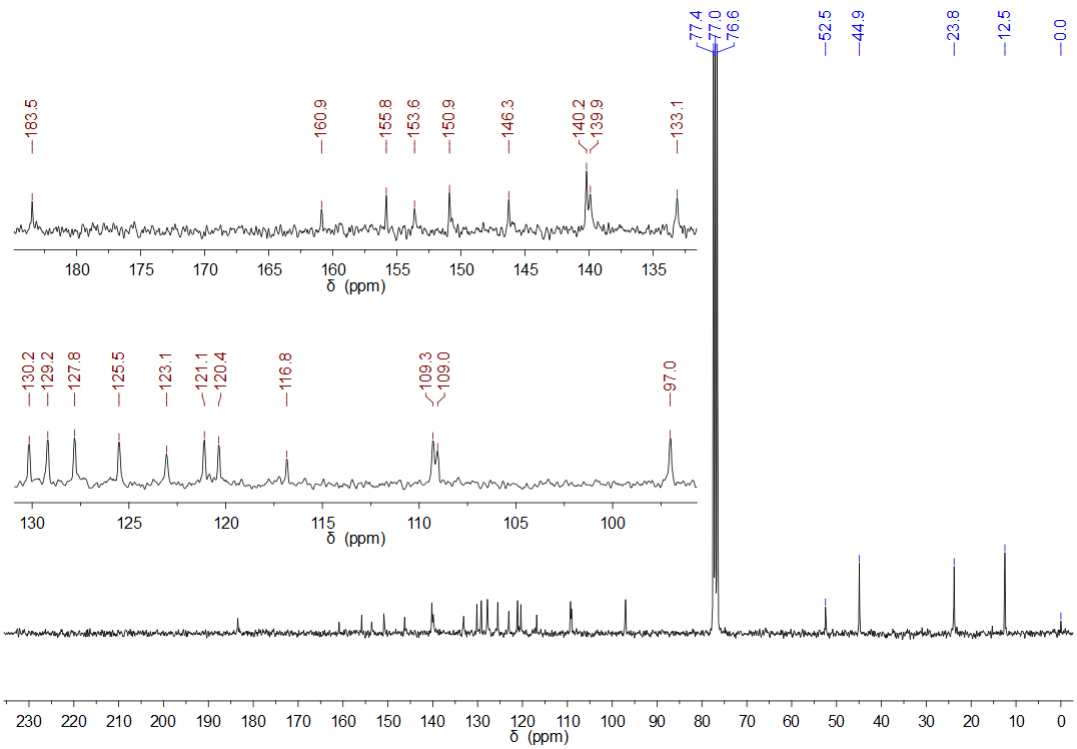

Fig. S20 ^{13}C NMR spectrum of **3** in $CDCl_3$.

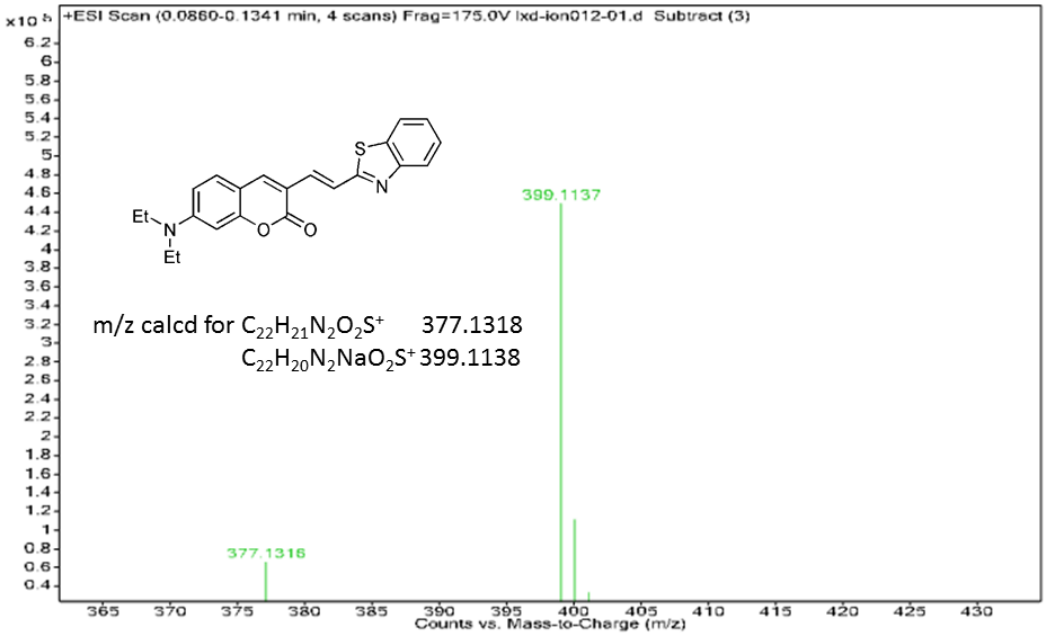

Fig. S21 Mass spectrum of **1**.

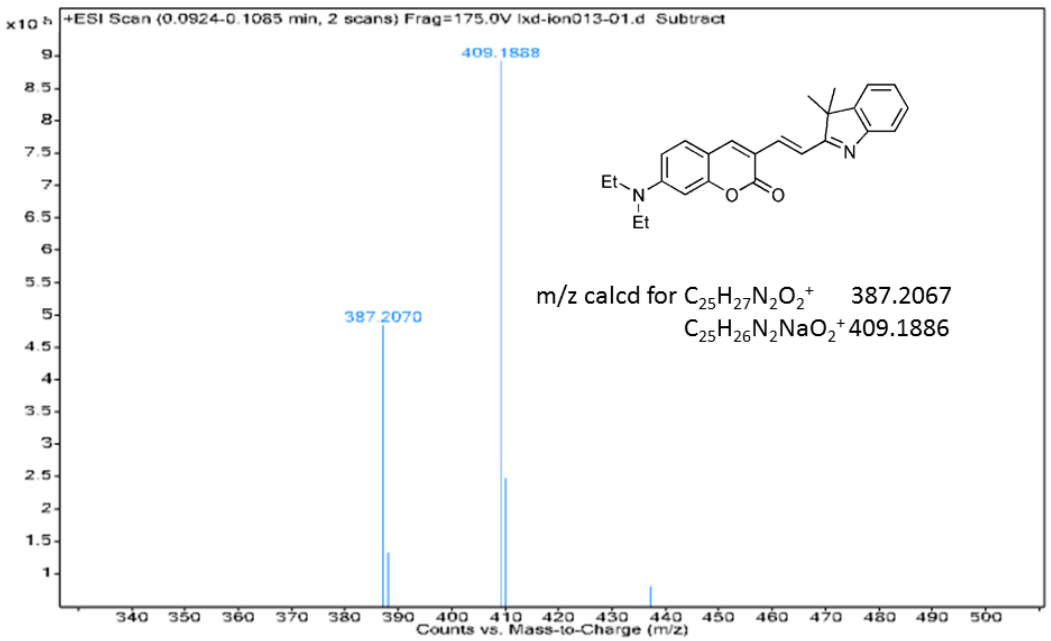

Fig. S22 Mass spectrum of **2**.

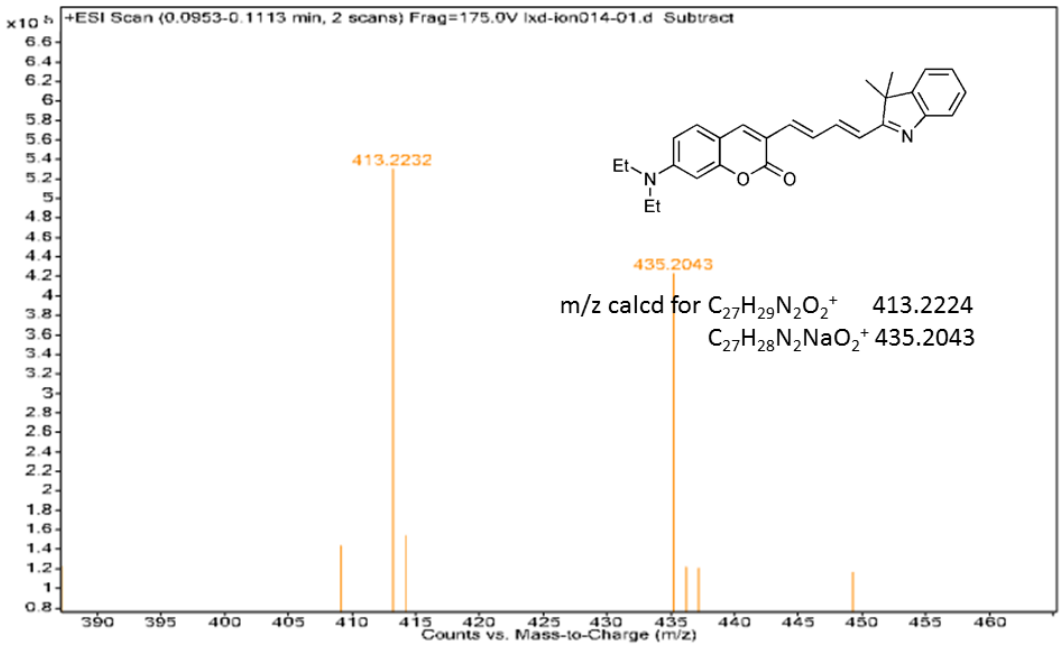

Fig. S23 Mass spectrum of **3**.